Available online at www.sciencedirect.com
SCIENCE DIRECT®
Journal of Nuclear Materials 337–339 (2005) 94–98
journal of nuclear materials
www.elsevier.com/locate/jnucmat

Model development and analysis of temperature-dependent lithium sputtering and sputtered Li^+ transport for tokamak plasma-facing applications

J.P. Allain [a,*], J.N. Brooks [a], D.A. Alman [b], L.E. Gonzalez [c]

[a] *Argonne National Laboratory, 9700 S Cass Ave, Argonne, IL 60439, USA*
[b] *University of Illinois at Urbana-Champaign, Urbana, IL, USA*
[c] *Departamento de Física Teórica, Universidad de Valladolid, Valladolid, Spain*

Abstract

We developed and applied models for overall (atom + ion) sputtering and sputtered Li^+ transport of liquid lithium tokamak divertor surfaces. The model/analysis has four parts: (1) a temperature-dependent data-calibrated empirical/code (TRIM) model of lithium sputtering by D^+ and Li^+ as a function of incident particle energy and angle; (2) temperature and energy-dependent molecular dynamics (MolDyn) modeling using an effective interionic pair potential of surface-reflected redeposited Li^+; (3) analytical model of reflected lithium charge state; and (4) analytic model of Li^+ near-surface emission/redeposition cascade. We predict: (1) strong temperature dependence of sputter yields, (2) reflection coefficients of order 50% (thermal energies) and 10% (hyperthermal energies), (3) reflected lithium charge fractions of 10–30% near 1 eV incidence, and (4) enhanced but non-runaway Li emission for the studied surface temperature range between 473 and 653 K.

PACS: 52.40.Hf; 52.55.Fa; 70.20.−m
Keywords: Liquid lithium; Sputtering; Low-energy reflection; Molecular dynamics

1. Introduction

Liquid lithium has been proposed as a divertor surface, e.g. [1,2], to help solve the critical plasma/surface interaction issues of erosion, heat and particle handling. Lithium is a unique plasma facing component (PFC) material in that most (∼2/3) sputtered particles will be Li^+*ions* [3], as opposed to ∼100% *atom* sputtering for solid materials (Be, C, W, etc.) and even other proposed liquids (Sn, Ga). For high heat flux PFC's (divertors, limiters), such sputtered ions will be intensely redeposited, within 1 μm from the surface, by the very strong plasma sheath normal electric field. The sputtered ions are thus essentially invisible to the plasma, and hence normally ignored in sputtering erosion and plasma contamination analysis. However, for rigorous calculations it is necessary to consider the *reflection* of said redeposited ions, as both ions and neutrals, and to model the resulting cascade process. In particular, we wish to determine conditions for a non-runaway reflection/redeposition process.

* Corresponding author. Tel.: +1 630 252 5184; fax: +1 630 252 3250.
E-mail address: allain@anl.gov (J.P. Allain).

0022-3115/$ - see front matter © 2004 Elsevier B.V. All rights reserved.
doi:10.1016/j.jnucmat.2004.10.144

Tokamak divertors generally have a geometry with near-oblique net magnetic field (~1–3° from the surface). In these cases the sheath region consists of a dual-structure ion-attracting magnetic sheath and debye sheath [4,5]. Considering the energy distribution of liquid lithium sputtered ions (peaking at <1–2 eV, and almost all less than $e\phi/4$), and typical values of near-surface electric and magnetic fields ($\sim 10^6$–10^7 V/m, and ~3–5 T respectively), almost all emitted (sputtered and reflected) Li^+ ions will be promptly redeposited at/near their origination point, with energy equal to their emitted energy, and with impingement angle (elevation) equal to their emitted angle. [1] This paper presents coupling of several code/models determining the net lithium atom erosion accounting for: lithium sputtering temperature-dependence, lithium ion self-reflection, and reflected lithium ion charge state fraction. Fits are made to experimental liquid-lithium (D-treated) data taken by Allain in the Ion-surface Interaction Experiment (IIAX) [6]. This set of models has been applied to NSTX presented in a paper by Brooks [7].

2. Semi-empirical model of temperature-dependent lithium sputtering

Experiments have measured lithium sputtering to remain under self-sputtering runaway levels for temperatures under ~673 K [6,8,9]. Lithium sputtering increases non-linearly with temperature for bombardment with D, He or Li ions between 543–673 K. Several models have attempted to explain this phenomenon [10,11]. In this work a semi-empirical model fits sputtering simulation runs with BCA (binary collision approximation) codes (e.g. TRIM [12]) calibrated to lithium sputtering experimental data.

The sputtering model consists of a semi-analytical temperature-dependent expression shown in Eq. (1) below based on work by Sigmund and Thompson [13–15].

$$Y(T) = C + A \cdot \exp(-B/T). \quad (1)$$

This model is fit to experimental and data-calibrated simulated data [16]. For the case of D and Li sputtering, energies range from 25 eV up to 10 keV as shown in Fig. 1. Temperatures studied are 473 and 653 K, although the models can be used at any desired temperature. Sputtered lithium ions (~2/3 of total) immediately return to the surface with energy equal to their sputtered energy (peaking at <1–2 eV). Sputtered energy distributions and angular sputtered distributions are calculated from the simulation codes. The empirical fits to the simulation data consist of the relation shown above in Eq. (1) where C is the parameter for the yield near the melting point of lithium at 473 K where the lithium sputtering yield remains invariant with temperature. This lithium yield obtained is for both neutrals and ions and used in the sputtered/reflected Li ion transport model. The constants A and B are fitting parameters.

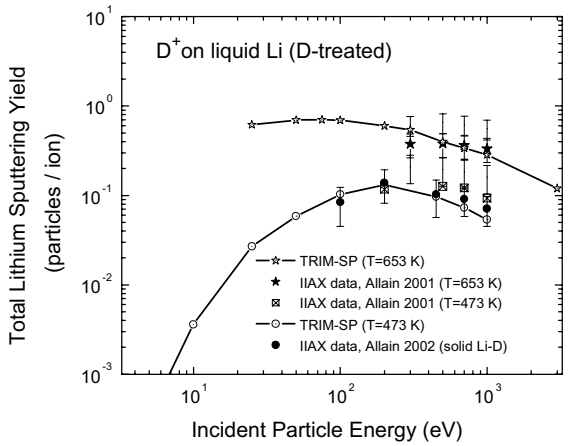

Fig. 1. TRIM-SP sputtering yield simulation data compared to IIAX temperature-dependent data plotted versus incident particle energy. Simulations are calibrated to experimental data by a special temperature-dependent model in the TRIM-SP code [16].

3. Atomistic simulations of low-energy Li^+ reflection from lithium

The MolDyn molecular dynamics code was used to simulate the lithium particle reflection from liquid lithium surfaces at low energies (thermal up to 100 eV). The potential used is an effective pair potential for liquid lithium obtained by Canales and Gonzalez [17–19] using the neutral pseudo-atom approximation (NPA) model [20]. Details of the MolDyn code used for liquid lithium are available in the literature [11,21,22]. For each lithium ion energy, the lithium self-reflection coefficient was run about 400 flights or histories.

The construction of the effective interionic pair potential for liquid lithium CGP (Canales–Gonzalez–Pardo) for simple metals is based on the use of pseudopotentials to describe the interaction between ions and valence electrons, and the application of first order and second order perturbation theory of a uniform electron gas in order to calculate the electronic density and the energy of the system respectively [20]. This approach is referred to as linear response theory (LRT). The resulting expression in Eq. (2) gives the

[1] This differs of course from the case for redeposited ions that result from ionization of emitted atoms, such ionization occurring much farther (≫1 μm) from the surface. In that case, as shown by codes such as REDEP/WBC [5], impingement velocity is completely different, with energies of about 5 kTe, and impingent angles of roughly 20–70°.

effective pair potential, $\phi(r)$, as a sum of the direct Coulomb repulsion between the ions of valence Z_v and an electron mediated part, $\phi_{ind}(r)$, whose Fourier Transform is obtained in terms of the pseudopotential $\tilde{v}_{ps}(q)$ and the response function of the uniform electron gas, $\chi(q)$ [17,19]

$$\phi r = \frac{Z_v^2}{r} + \phi_{ind}(r),$$
$$\tilde{\phi}_{ind}(r) = \chi(q)\left[\tilde{v}_{ps}(q)\right]^2. \quad (2)$$

This effective pair potential with use of the pseudopotential described in detail in the references, was found to properly describe most properties of liquid lithium [20].

4. Results

4.1. Lithium reflection simulations

The lithium reflection coefficient, R, is calculated as a function of incident particle energy at 473 and 653 K at 20° incidence, shown in Fig. 2. Three distinct regions are found in the dependence of R with energy. A 'high-energy' region that begins near 20 eV or more, a hyperthermal region that extends from 0.1 eV up to about 10 eV and a thermal region that ranges from ambient temperature near 0.026 eV up to about 0.1 eV. Surface atoms appeared quite mobile at both temperatures simulated. Reflection of lithium particles averaged about 1–4% for system temperatures at 473 and 653 K and energies equal to 20 eV. This is expected since large incident particle energies lead to particles penetrating many monolayers deep within liquid lithium. For energies higher than 20 eV, the reflection coefficient decreases rapidly.

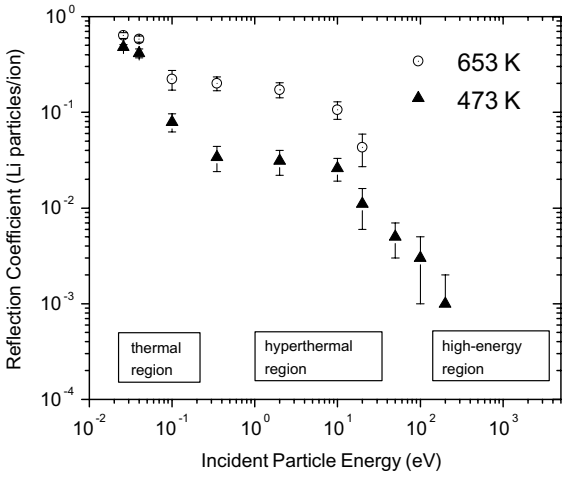

Fig. 2. Molecular dynamics results of lithium self-bombardment reflection as a function of incident lithium particle energy for 453 K and 653 K system temperatures. Simulations are done for 20-degree incidence and average 300–400 flights.

As the energy of the incident particle is lowered the reflection coefficient reaches a plateau where the coefficient is nearly constant with incident particle energy. This plateau is associated with incident atoms which had sufficient energy to penetrate about 1–2 monolayers and were not able to overcome the activation desorption barrier. About 50–60% of the incident lithium ions at energies between 0.0259–0.04 eV backscattered from the mobile liquid lithium surface within the simulation time of up to 1 psec. The reason for such a strong dependence on surface temperature is the electron density dependence on temperature in the inter-atomic potential used for liquid lithium. Work on feasibility of this potential to simulate the liquid-metal *surface* of liquid lithium is continuing [23] and further results on its effect on reflection coefficient will be presented in future work.

4.2. Semi-analytical model of Li^+ charge dynamics during reflection from lithium

The ion probability for *backscattered* lithium particles is analyzed in this section. This is done by a semi-analytical study coupled to molecular dynamics simulations of the scattering trajectories of incident lithium particles described earlier.

Non-adiabatic charge fractions of backscattered and sputtered alkali atoms have been observed to depend strongly on their outgoing velocity from the surface and such observations are in good qualitative agreement with theory [24]. Resonant charge exchange is active in the backscattering and sputtering of alkali atoms from alkali metal surfaces due to alkali ionization potentials being comparable to the alkali metal work functions. This is quite different from noble gas ion scattering from surfaces, which typically undergo a high rate of irreversible Auger neutralization (high ionization potential) and thus their backscattering ionization probabilities are nearly zero.

The dominant charge transfer mechanism in the backscattering of alkali ions (e.g. lithium) from metallic surfaces is resonant charge transfer [25]. As the ion approaches the metallic surface the ionization level of the incident atom is raised by the image potential. In addition to this effect, the ionization level is broadened into a resonance with a spatially dependent width, $\Delta(z)$ [26–30]. The ionization probability is defined as

$$P^+ = \exp\left[\frac{-2\Delta(z_c)}{\hbar\alpha v_p}\right], \quad (3)$$

$\Delta(z_c)$ is the resonance width of the ionization level at the distance from the surface where it crosses the Fermi level, z_c in units of Å. In the expression above, α is the characteristic decay length for the rate at which the ionization level width of emitted ions decreases as their distance from the surface, z, increases in units of m^{-1} and

v_p is the component of the outgoing velocity of the alkali ion perpendicular to the surface in m/sec.

Since there is a strong dependence of the ion probability on the velocity distribution of backscattered or sputtered alkali atoms, molecular dynamics simulations discussed earlier are used to obtain the outward lithium particle velocity and angle. The ionization probability therefore is an average probability defined as

$$P^{+}_{\text{total}} \equiv \sum_{N=1}^{100} \frac{P^{+}_{N}(v_p(\Theta))}{N}, \tag{4}$$

where the probability is calculated at each flight, N, having a particular v_p with angular direction dependence, Θ, calculated by MolDyn. Fig. 3 shows the results for the ion probability of reflected lithium ions at system temperature of 473 and 653 K. The ion probability for thermal and hyperthermal energies is quite low as expected since the backscattered ion spends a longer time near the surface with a higher probability of neutralizing the emitted ion.

4.3. Sputtered/reflected ion transport model

Rigorous analysis of the transport of surface-emitted material in a plasma can be made using coupled plasma, sputtering, molecular-dynamic, sheath, and impurity transport codes. A simple parametric model can be used here to scope out the lithium ion sputtering/reflection cascade issue. We are interested in the net surface emission of lithium atoms resulting from lithium ion recycling. We use parameters: Y is (total) lithium sputtering coefficient (lithium ions and atoms sputtered per incident deuterium ion) from the temperature-dependent model, ε' is the charge fraction of sputtered lithium, R is the reflection coefficient of sheath-redeposited Li^+ and ε is the charge fraction of reflected lithium. Considering the initially sputtered material and the successive redeposition/reflection stages, the 'effective atom sputtering coefficient, Y_o^{eff}' = ratio of total emitted (sputtered plus reflected) lithium atom flux to incident deuterium ion flux, is given by

$$Y_o^{\text{eff}} = (1-\varepsilon')Y + \varepsilon'(1-\varepsilon)RY + \varepsilon'(1-\varepsilon)R^2\varepsilon Y + \varepsilon'(1-\varepsilon)R^3\varepsilon^2 Y + \ldots, \tag{5}$$

which sums to

$$Y_o^{\text{eff}} = Y\left[1-\varepsilon'+\varepsilon'(1-\varepsilon)\frac{R}{1-\varepsilon R}\right]. \tag{6}$$

We use here a value of $\varepsilon' = 2/3$ for the sputtered lithium charge fraction since it is weakly dependent on temperature [6]. Then using typical parameter values from the above calculations, for a range of low emitted/incident energies 0.1–2 eV, we obtain the lithium atom sputtering amplification factor (Y_o^{eff}/Y), shown in Table 1 and Fig. 4. Considering the typical sputtered energy of order 1 eV, at 473 K there is little enhancement of net atom sputtering. At 653 K, however, the total lithium atom flux to the plasma is about 30% greater than computed

Table 1
Results for lithium atom sputtering amplification factor for 473 and 653 K for a 2 eV sputtered Li ion from D-bombardment near 200 eV

Lithium surface temperature (K)	R	ε	Y_o^{eff}/Y
473	0.031	0.11	0.358
653	0.172	0.12	0.443

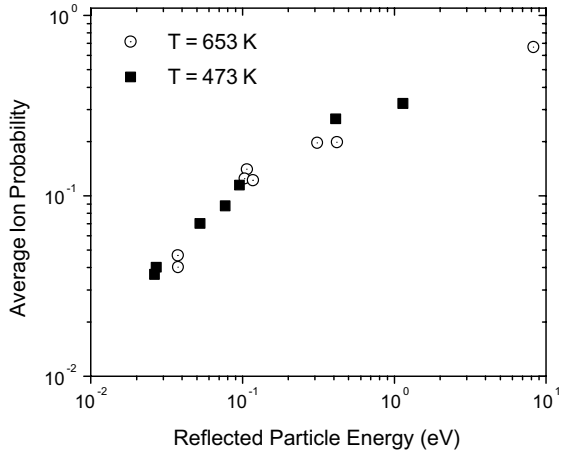

Fig. 3. Average ion probability of backscattered lithium particles at incident energies ranging from 0.0259 eV and 20 eV. System temperatures shown are for 473 and 653 K.

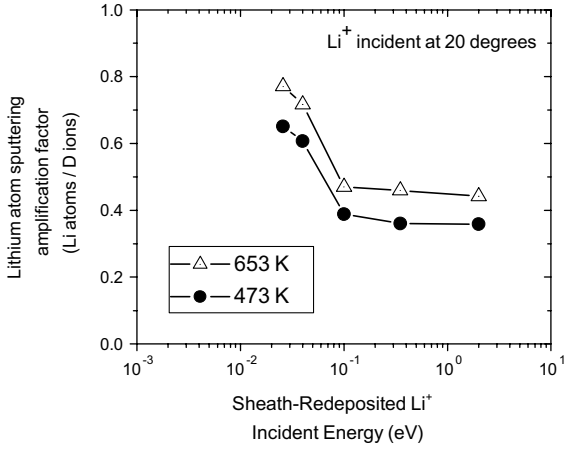

Fig. 4. The lithium atom sputtering amplification factor, which is the ratio of total emitted lithium atoms to incident deuterium ion flux, plotted for 473 and 653 K against the sheath-redeposited Li^+ incident energy.

by not considering the reflection process (i.e., ~0.44 vs. ~0.33), but is well short of runaway. An important future assessment to make is the behavior at higher surface temperatures, specifically near the upper limit of feasible lithium operation of 723–773 K.

5. Conclusions

A semi-empirical temperature-dependent model for lithium erosion has been developed based on scaling law models by Sigmund and Thompson. Lithium self-reflection and its charged state were calculated with atomistic simulations using an effective interionic pair potential for liquid lithium developed by Gonzalez et al. [20]. Molecular dynamics results gives reflection coefficients up to about 50% for thermal energies and 10% for hyperthermal energies. Ion probabilities range from 10–20% for energies between 0.1–1.0 eV. Further assessment is needed whether the lack of simulating liquid-metal stratification and smoothness has a strong effect on lithium ion reflection studied here. The analytical sputter/redeposition/reflection cascade model developed here can be used to assess surface temperature non-runaway limits. We find enhanced but stable operation of a liquid lithium divertor system for the temperatures studied.

Acknowledgment

Work supported by the US Department of Energy – Office of Fusion Energy Sciences.

References

[1] J.N. Brooks, Overview of the ALPS program, presented at the 16th Topical Meeting on the Technology of Fusion Energy, Madison, WI, 2004. Fus. Sci. Technol., submitted for publication.
[2] R.F. Mattas et al., Fus. Eng. Design 49&50 (2000) 127.
[3] J.P. Allain, D.N. Ruzic, Nucl. Fus. 42 (2002) 202.
[4] T.Q. Hua, J.N. Brooks, Phys. Plasmas 1 (11) (1994) 3607.
[5] R. Chodura, Phys. Fluids 25 (1990) 1628.
[6] J.P. Allain, Ph.D., University of Illinois at Urbana-Champaign, 2001.
[7] J.N. Brooks et al., these Proceedings. doi:10.1016/j.jnucmat.2004.07.062.
[8] R.P. Doerner et al., J. Nucl. Mater. 313–316 (2003) 385.
[9] R.W. Conn et al., Nucl. Fus. 42 (2002) 1060.
[10] R.P. Doerner et al., these Proceedings.
[11] J.P. Allain et al., Nucl. Instrum. and Meth. B, submitted for publication.
[12] J.P. Biersack, W. Eckstein, J. Appl. Phys. A 34 (1984) 73.
[13] P. Sigmund, in: R. Behrisch (Ed.), Sputtering by Particle Bombardment I, Springer-Verlag, Berlin, 1981.
[14] M.W. Thompson, Vacuum 66 (2002) 99.
[15] P. Sigmund, M. Szymonski, Appl. Phys. A: Solids Surf. 33 (1984) 141.
[16] J.P. Allain, M.D. Coventry, D.N. Ruzic, J. Nucl. Mater. 313–316 (2003) 645.
[17] M. Canales, L.E. Gonzalez, J.A. Padro, Phys. Rev. E 50 (5) (1994) 3656.
[18] L.E. Gonzalez, D.J. Gonzalez, M. Canales, Z. Phys. B 100 (1996) 601.
[19] M. Canales et al., J. Phys.: Condens. Matter 5 (1993) 3095.
[20] L.E. Gonzalez et al., J. Phys.: Condens. Matter 5 (1993) 4283.
[21] D.A. Alman, D.N. Ruzic, J. Nucl. Mater. 313–316 (2003) 182.
[22] K. Beardmore, R. Smith, Nucl. Instrum. and Meth. B 106 (1995) 74.
[23] Z. Insepov, A. Hassanein, J. Nucl. Mater., these Proceedings.
[24] J.W. Rabalais (Ed.), Principles and Applications of Ion Scattering Spectrometry, John Wiley, New York, 2003.
[25] M. Shi, O. Grizzi, J.W. Rabalais, Surf. Sci. 235 (1990) 67.
[26] G.A. Kimmel et al., Phys. Rev. B 43 (12) (1991) 9403.
[27] R. Brako, D.M. Newns, Rep. Prog. Phys. 52 (1989) 655.
[28] R. Brako, D.M. Newns, Surf. Sci. 108 (1981) 253.
[29] M.L. Yu, in: R. Behrisch, K. Wittmaack (Eds.), Sputtering by Particle Bombardment III, 64, Springer-Verlag, Berlin, 1991.
[30] H. Gnaser, in: G. Höhler (Ed.), Low-energy Ion Irradiation of Solid Surfaces, Springer-Verlag, Berlin, 1999.